Thermodynamic Effects of the Hydrophobic Surfactant Proteins on the Early Adsorption of Pulmonary Surfactant

Vincent Schram and Stephen B. Hall

Departments of Biochemistry and Molecular Biology, Medicine, and Physiology and Pharmacology, Oregon Health and Science University, Portland, Oregon 97201-3098 USA

ABSTRACT We determined the influence of the two hydrophobic proteins, SP-B and SP-C, on the thermodynamic barriers that limit adsorption of pulmonary surfactant to the air–water interface. We compared the temperature and concentration dependence of adsorption, measured by monitoring surface tension, between calf lung surfactant extract (CLSE) and the complete set of neutral and phospholipids (N&PL) without the proteins. Three stages generally characterized the various adsorption isotherms: an initial delay during which surface tension remained constant, a fall in surface tension at decreasing rates, and, for experiments that reached ~40 mN/m, a late acceleration of the fall in surface tension to ~25 mN/m. For the initial change in surface tension, the surfactant proteins accelerated adsorption for CLSE relative to N&PL by more than ten-fold, reducing the Gibbs free energy of transition ($\Delta G_0^{\ddagger}$) from 119 to 112 kJ/mole. For the lipids alone in N&PL, the enthalpy of transition ($\Delta H_0^{\ddagger}$, 54 kJ/mole) and entropy ($-T \cdot \Delta S_0^{\ddagger}$, 65 kJ/mole at 37°C) made roughly equal contributions to $\Delta G_0^{\ddagger}$. The proteins in CLSE had little effect on $-T \cdot \Delta S_0^{\ddagger}$ (68 kJ/mole), but lowered $\Delta G_0^{\ddagger}$ for CLSE by reducing $\Delta H_0^{\ddagger}$ (44 kJ/mole). Models of the detailed mechanisms by which the proteins facilitate adsorption must meet these thermodynamic constraints.

INTRODUCTION

Pulmonary surfactant contains two very hydrophobic proteins, SP-B and SP-C, that are critical for normal respiration. The lungs require a thin film of surfactant to stabilize the small alveolar air spaces by reducing surface tension, and these proteins ensure that the film forms quickly. They greatly increase the rate at which simple model systems of surfactant lipids adsorb to an air–liquid interface (Whitsett et al., 1986; Hawgood et al., 1987; Warr et al., 1987; Arjomaa and Hallman, 1988; Yu and Possmayer, 1990; Oosterlaken-Dijksterhuis et al., 1991a). With the complete set of lipids in native surfactant, they accelerate adsorption by at least an order of magnitude (Wang et al., 1996). Rapid adsorption is essential. In humans (Nogee, 1998) or transgenic animals (Tokieda et al., 1997) that lack these proteins, respiratory failure occurs soon after birth. Other functions have been proposed for these proteins (Longo et al., 1993; Taneva and Keough, 1994a,b,c; Wang et al., 1995; Lipp et al., 1996; Galla et al., 1998; Kruger et al., 1999; Veldhuizen and Haagsman, 2000), but their ability to promote adsorption represents their best defined activity.

The studies reported here address the effects of the hydrophobic proteins on the rate-limiting barrier to adsorption in two respects. We deal first with the extent to which the proteins alter each of the thermodynamic components, enthalpy and entropy, of the activation barrier. For complete surfactant, a prior study indicates that the barrier is primarily entropic (King and Clements, 1972). The change produced by the proteins, however, on the barrier faced by vesicles containing only the lipids remains unknown. We also address the second issue of the extent to which the proteins convert adsorption to a diffusion-limited process. For a surfactant that faces no activation barrier limiting its insertion into the interface, the rate of adsorption is instead determined by transport to the surface (Ward and Tordai, 1946; Defay and Pétré, 1971; Borwankar and Wasan, 1983; Johannsen et al., 1991; Dukhin et al., 1995; Liggieri et al., 1996). To begin addressing the mechanisms by which the proteins promote adsorption, we determine here their effect on the different components of the energy barrier and the extent to which they convert adsorption to a diffusion-limited process.

MATERIALS AND METHODS

Materials

Extracted calf surfactant (calf lung surfactant extract, CLSE [Notter et al., 1983]) was provided by Dr. Edmund Egan (ONY Inc., Amherst, NY). All chemicals used were of analytical grade. Solvents were of spectroscopic grade. Distilled water passed through a multicartridge purification system (Barnstead, Dubuque, IA) had a resistivity greater than 17.3 MΩ/cm. Our standard buffer contained 150 mM NaCl, 1.5 mM $CaCl_2$, 10 mM Hepes pH 7.0 (HSC).

N&PL purification

The hydrophobic components of CLSE were fractionated by gel permeation chromatography (Hall et al., 1994). Peaks containing the phospholipids and cholesterol were pooled to obtain the neutral and phospholipids (N&PL). This procedure reduces the protein content from 10 μg/μmol phospholipid for CLSE to undetectable levels below 0.5 μg/μmol phospholipid for N&PL (Hall et al., 1994).

Received for publication 1 March 2001 and in final form 15 May 2001.

Address reprint requests to Stephen B. Hall, Molecular Medicine, M/C NRC-3, OHSU, Portland, OR 97201-3098. Tel.: 503-494-6667; Fax: 503-494-6670; E-mail: sbh@ohsu.edu.

0006-3495/01/09/1536/11 $2.00

Methods

Biochemical assays

Phospholipid concentrations were determined by phosphate assay (Ames, 1966). Protein content was assayed with amido black on material precipitated with trichloroacetic acid (Kaplan and Pedersen, 1989). Total cholesterol was assayed by reduction with ferrous sulfate (Searcy and Bergquist, 1960).

Suspension of vesicles

Lipids were dispersed by sonication. Chloroform solutions containing the desired amounts of lipid were deposited in a test tube and the solvent evaporated under a stream of nitrogen. After extensive vortexing in 1 ml HSC buffer, the lipids were then sonicated for 10 min with a probe sonicator (Branson, Danbury, CT) at 10-W output. Sonication was carried out on ice to minimize lipid degradation (Notter et al., 1983). The resulting vesicles were kept at room temperature and used over a period of 8–10 h without noticeable change in turbidity or adsorption kinetics. The diffusion coefficients of vesicles were measured using dynamic light scattering (DynaPro LSR, Protein Solutions, Inc., Charlottesville, VA) at ambient temperatures and then calculated for other temperatures assuming the Stokes–Einstein relationship and a constant hydrodynamic radius.

Measurements of surface tension

Surface tension was measured using a 1-cm-wide Wilhelmy paper plate attached to a home-build force transducer consisting of a flat spring connected to a displacement transducer (Omega Engineering, Stamford, CT). The signal was amplified by a digital signal meter (70701, Oriel, Stratford, CT) and recorded via I/O board (National Instruments, Austin, TX) to computer (Quadra, Apple Inc., Cupertino, CA) using the graphical interface program LabVIEW (National Instruments). The transducer was calibrated in surface tension using known weights.

We measured adsorption as a function of time following removal of the surface film from above a suspension of vesicles (King and Clements, 1972). A Teflon beaker with 3.2 cm^2 cross-section (Baxter Scientific Products, McGaw Park, IL) contained 5 ml HSC buffer within a temperature-controlled humidity-saturated chamber. The lower edge of the Wilhelmy plate was positioned a few millimeters below the interface. The desired quantity of vesicles was introduced through the air–water interface using a Hamilton syringe before stirring the subphase for 10 min. The interface was then cleaned with a Pasteur pipette connected to a water aspirator until surface tension reached the value expected for pure water (70 mN/m at 37°C), a process that typically required less than 5 s. Adsorption isotherms (surface tension versus time) were then recorded over a period of 35 min. Selected experiments performed in triplicate obtained surface tensions that were reproducible to within 5%.

Calibration of surface concentration

Conversion of measured surface tension to surface concentration required isotherms relating the two variables. Similar to most previous kinetic studies that have used surface tension to follow adsorption, our analysis assumes a unique relationship between surface tension and surface concentration for each preparation. Isotherms were generated by depositing known amounts of CLSE or N&PL in chloroform solution at the surface of 5 ml HSC in the Teflon cup and measuring the surface tension of the resulting film. Experiments were performed in triplicate and the results averaged. The plots of surface tension versus surface concentration (not shown) were linear between 68 and 32 mN/m (r^2 = 0.974 for CLSE and 0.971 for N&PL), and the equations for the least-squares fit were used in each case to provide the required conversion. CLSE films formed by spreading and by adsorption followed the same isotherm when compressed from low surface pressures.

The calibration isotherms also provided a sensitive method for confirming that aspiration of the surface completely removed the interfacial film. Following a series of sequential depositions to construct a calibration curve, the surface was cleaned by our standard procedure, and the depositions repeated. The exact reproduction of the original isotherm following each of three sequential iterations of aspiration and deposition confirmed that no material accumulated at the surface, and that our procedure produced a clean interface.

RESULTS

We compared the kinetics of adsorption for N&PL, which contains the complete set of surfactant lipids from calves, and for CLSE with the hydrophobic proteins SP-B and SP-C in addition to the same set of lipids (Hall et al., 1994). Determination of the thermodynamic barriers to adsorption for each preparation required measurement of the rate constants at a series of different temperatures. The rate constants in turn required information on the order of the reaction, which was obtained from measurements of adsorption at different concentrations. We followed the kinetics by measuring surface tension with time after removal of the interfacial film from above a dispersion of vesicles (King and Clements, 1972). Experiments were conducted at temperatures that varied by 5°C increments between 10°C and 50°C. At each temperature, measurements were obtained at six concentrations over the range from 10 to 250 μM (Figs. 1 and 2 for N&PL and CLSE, respectively).

The adsorption curves demonstrated three characteristic features (Figs. 1 and 2). Surface tension remained constant for a variable initial delay before deviating from the value for a clean interface. Surface tension then fell during a second phase at variable but progressively slower rates to ~40–45 mN/m. For experiments that reached these surface tensions during the 35-min experiments, adsorption then accelerated during the third phase before reaching final constant values of approximately 25 mN/m.

Our analysis emphasized the relatively simple early stages of adsorption when the subphase vesicles encounter an interface with little pre-existing material. We characterized these initial stages in terms of two variables: the lag time between the start of the experiment and the first measurable change in surface tension; and the slope of the surface tension–time isotherm during the initial fall in surface tension. The isotherms were linear for at least the initial 5 mN/m drop in surface tension for all experiments. The relationship of surface tension to surface concentration determined in separate experiments was also linear, and so the rates at which surface tension fell could be converted directly to rates at which material adsorbed to the interface. The duration of the initial delay (Fig. 3) correlated inversely with the initial rate of ad-

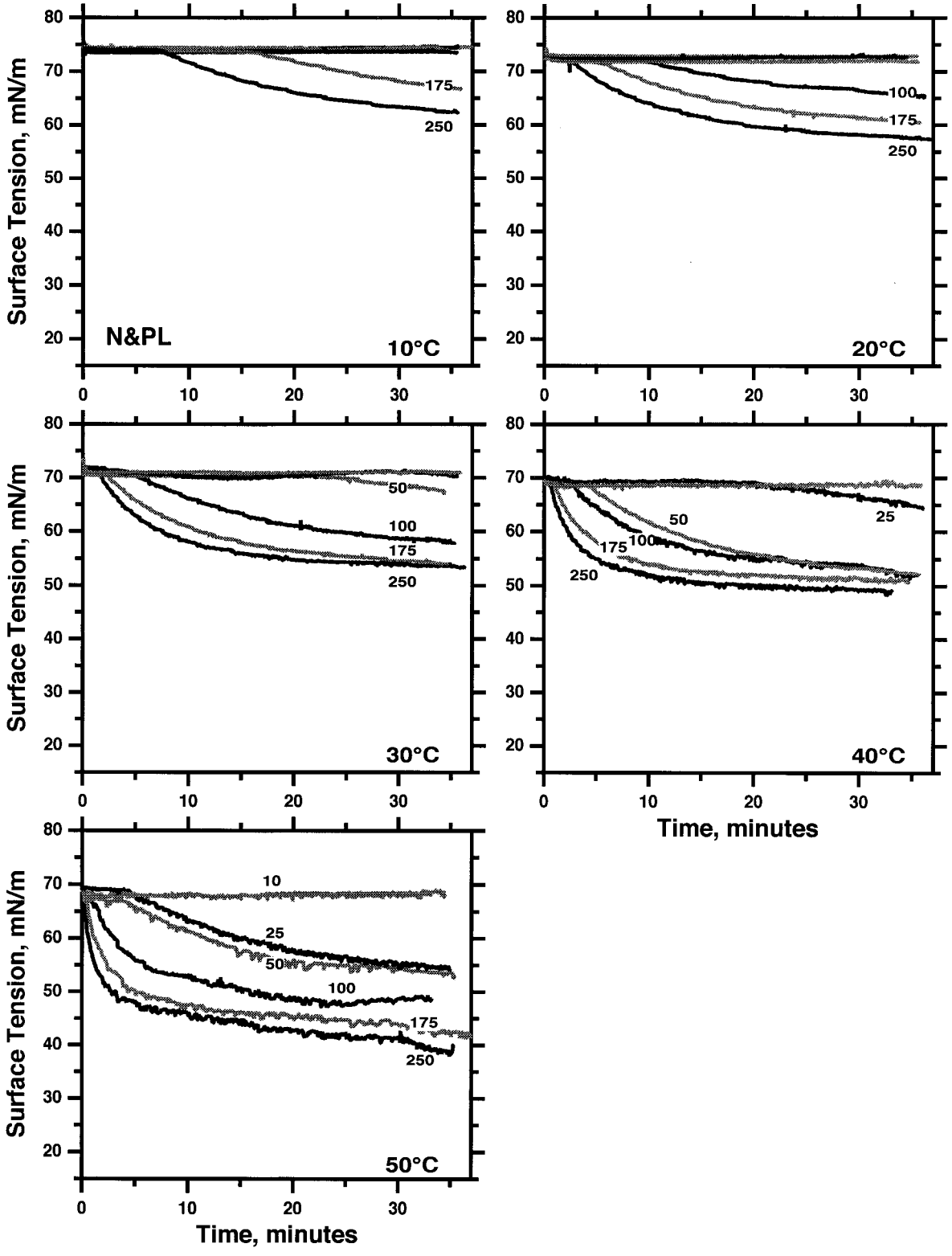

FIGURE 1 Adsorption of N&PL vesicles to a clean air–water interface. The concentration of N&PL in the subphase is indicated in μM phospholipid on each curve, and temperature is specified on each graph. Data obtained at 15°C, 25°C, 35°C, and 45°C are omitted for the sake of clarity.

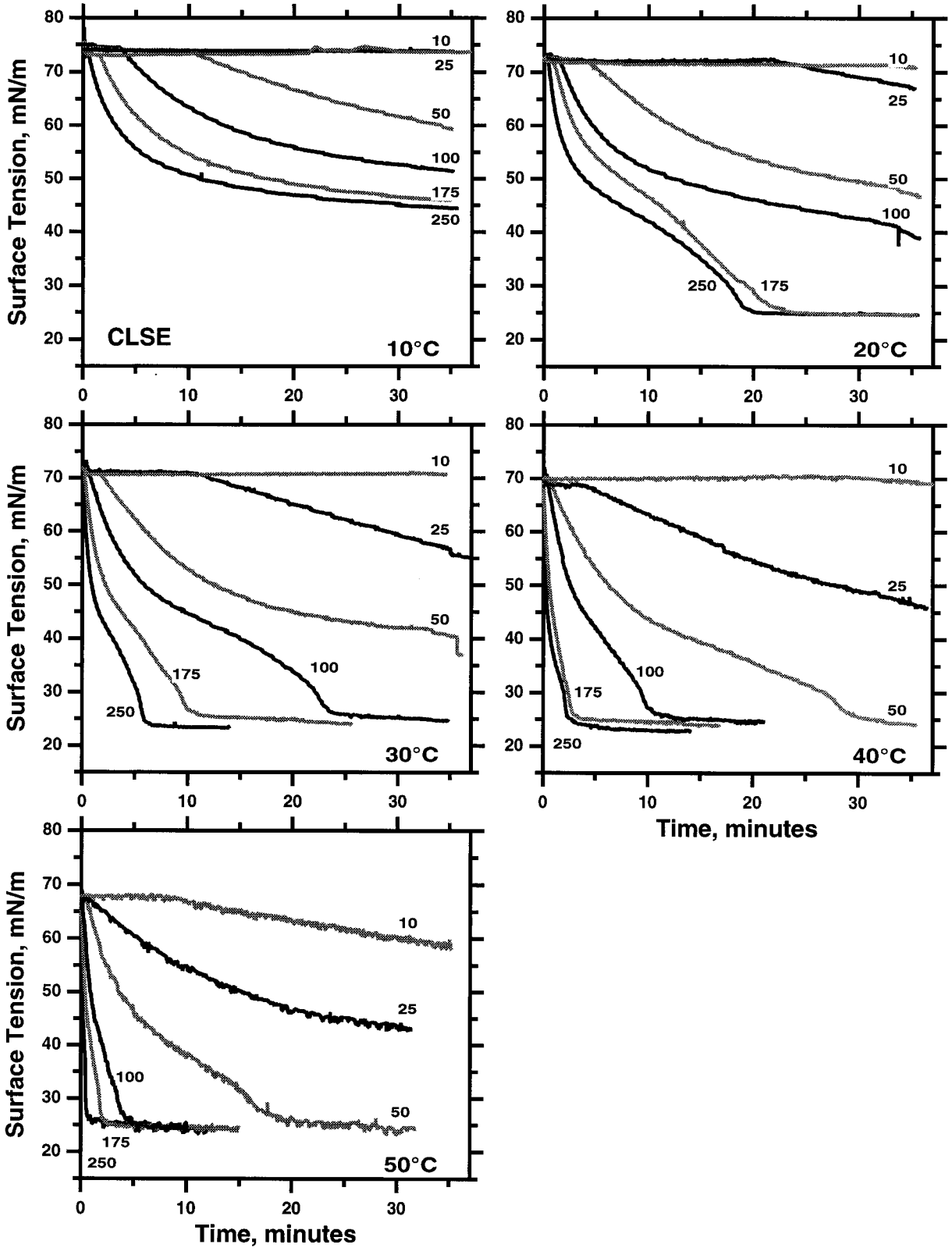

FIGURE 2 Adsorption of CLSE vesicles to a clean air–water interface. The concentration of CLSE in the subphase is indicated in μM phospholipid on each curve, and temperature is specified on each graph. Data obtained at 15°C, 25°C, 35°C, and 45°C are omitted for the sake of clarity.

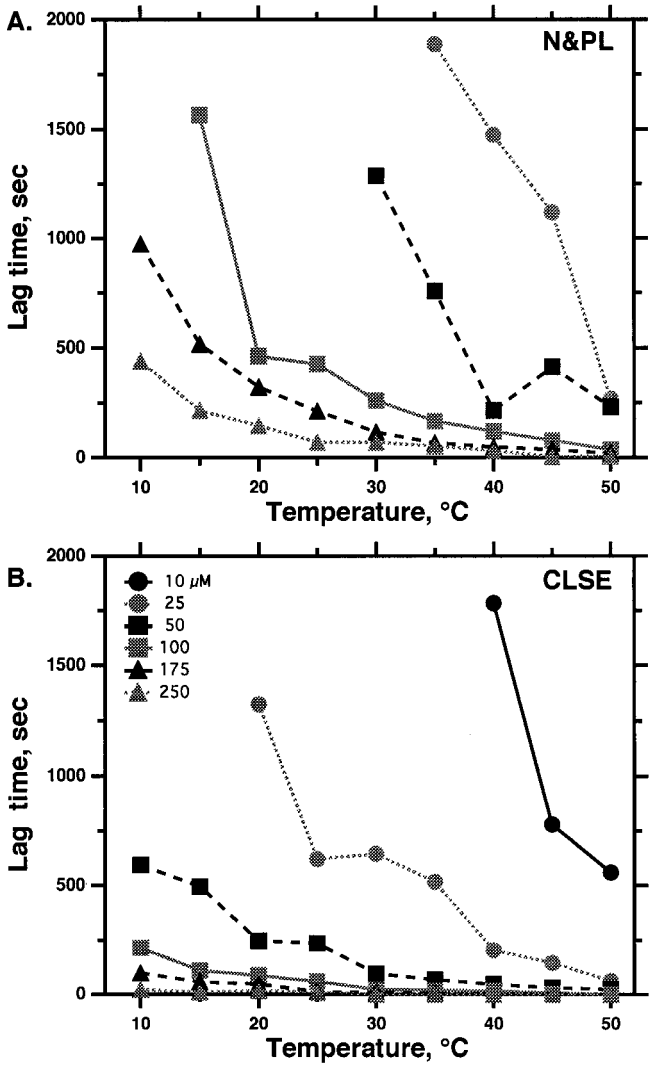

FIGURE 3 Lag time between formation of a clean interface and detection of a change in surface tension. (*A*) N&PL. (*B*) CLSE. The absence of a value reflects no measurable adsorption within the 35-min experiment.

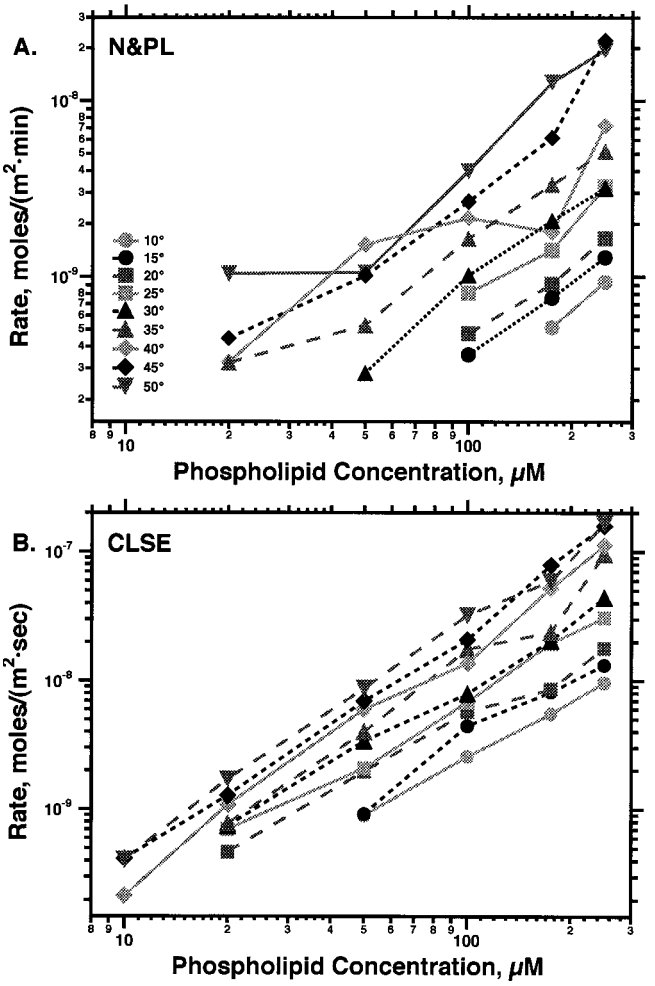

FIGURE 4 Rates of initial adsorption. The slope during the initial reduction in surface tension was converted from mN/(m · sec) to mole/(m^2 · sec) using isotherms relating surface tension to surface concentration (see Methods). Absent data indicate conditions at which no change in surface tension occurred during the 35-min experiment. (*A*) N&PL. (*B*) CLSE.

sorption (Fig. 4). Higher temperatures, higher concentrations, and the presence of the surfactant proteins in CLSE relative to N&PL all produced faster initial rates and shorter delays. The lag phase became inapparent when the initial rate exceeded a certain level, presumably because it became undetectably short.

The thermodynamic calculations required determination of k_m, the measured reaction rate constant, from the initial rate. This in turn required n, the order of the reaction, according to the equation

$$\text{rate} = k_m \cdot c^n$$

for a concentration c in the bulk phase. Linear fits of logarithmic plots for initial adsorption rates versus concentration had slopes that varied little with temperature (Fig. 4). The slopes for both preparations were >1, indicating a process other than first order. The apparent reaction order was 1.4 ± 0.2 for N&PL and 1.7 ± 0.2 for CLSE. These average values of n were then used to obtain the kinetic rate constants k_m from the initial adsorption rates at the different temperatures.

To determine the extent to which the rate of adsorption for each preparation was determined by diffusion, we compared k_m with k_d, the calculated rate constant for adsorption limited by diffusion. Measurements with dynamic light scattering provided values of D, the diffusion coefficient. We then used the equation of Ward and Tordai (1946) that relates surface concentration (Γ) to time (t) for diffusion-limited adsorption:

$$\Gamma = 2c \cdot \left(\frac{Dt}{\pi}\right)^{1/2}.$$

This expression ignores a second term in the original equation for back-diffusion in the interests of simplicity, and because

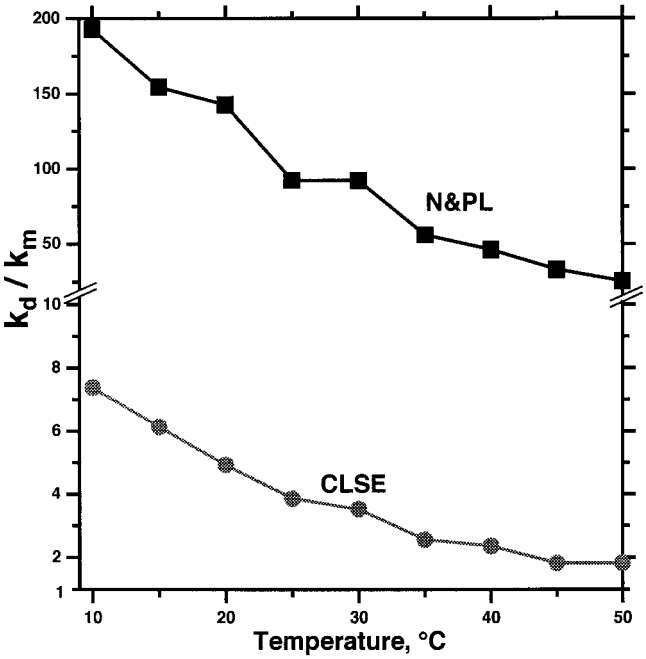

FIGURE 5 Comparison of measured kinetics to a diffusion-limited process. k_d is the calculated rate constant for a diffusion-limited process (Ward and Tordai, 1946; and k_m is the measured rate constant. Axis of ordinates is broken to demonstrate the behavior of both preparations more clearly.

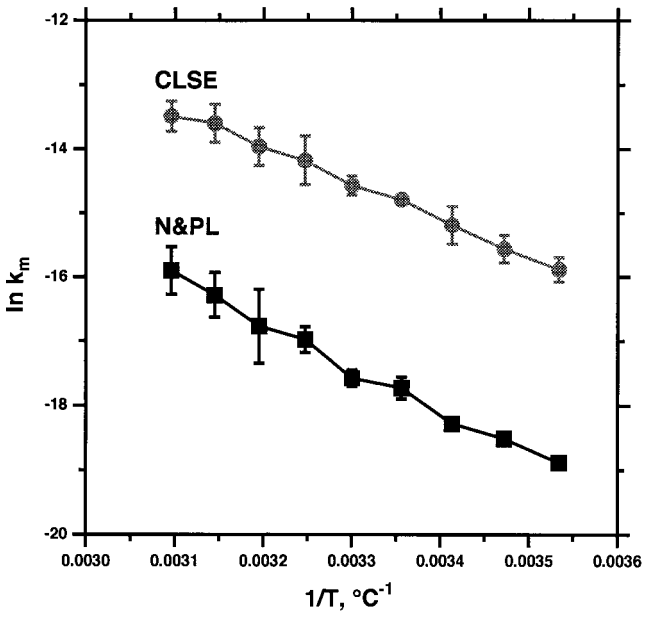

FIGURE 6 Arrhenius plots for adsorption during the initial reduction in surface tension. The slope of linear regressions provide E_a, the energy of activation. k_m is the measured rate constant for adsorption during the initial fall in surface tension, expressed as mean ±SD averaged over measurements at six concentrations. Error bars are obscured by the symbols in some cases.

initial adsorption when the interfacial and subsurface concentrations are low may minimize that process. Differentiation and substitution to obtain an expression in Γ yields

$$\frac{d\Gamma}{dt} = \left(\frac{2D}{\pi\Gamma}\right) \cdot c^2,$$

so that

$$k_d = \frac{2D}{\pi\Gamma}$$

for diffusion-limited adsorption at any surface concentration Γ. A surface tension of 65 mN/m corresponded to a molecular area of ~83 Å^2/molecule and a surface concentration of 2 μmole/m^2 for both N&PL and CLSE, and k_d was calculated at that point. Light scattering measurements provided values of D at ambient temperatures, and the Stokes–Einstein relationship,

$$D = \frac{k_b T}{6\pi\eta r}$$

allowed calculation of values at other temperatures. k_b is the Boltzmann constant, η is the viscosity of the solvent, and r is the hydrodynamic radius. Values of r at ambient temperatures were 57 ± 11 and 73 ± 9 nm for vesicles of N&PL and CLSE, respectively and were assumed constant at other temperatures.

The ratio of k_d to k_m provided an indication of the extent to which adsorption became diffusion limited. For both N&PL and CLSE, k_d/k_m fell with increasing temperature (Fig. 5). For N&PL, the ratio remained above 10 at all temperatures, indicating that the actual process was at least an order of magnitude slower than predicted for diffusion-limited adsorption. The additional presence of the proteins in CLSE, however, reduced the ratio substantially, and, above 40°C, the rate was only twice that of the diffusion-limited process.

The slopes from the Arrhenius plots of $\ln k_m$ versus $1/T$ (Fig. 6) provided activation energies E_a according to the equation

$$\ln k_m = -\frac{E_a}{R} \cdot \frac{1}{T} + \ln A,$$

where R is the gas constant and A is the Arrhenius pre-exponential factor. Transition-state theory considers the effect of temperature in terms of an equilibrium between reactants and an activated complex (Eyring, 1935). Consequently,

$$k_m = \frac{k_b T}{h} \cdot e^{-\Delta G_0^{\ddagger}/RT}$$

$$\ln \frac{k_m}{T} = -\frac{\Delta G_0^{\ddagger}}{R} \cdot \frac{1}{T} + \ln \frac{k_b}{h}$$

$$= -\frac{\Delta H_0^{\ddagger}}{R} \cdot \frac{1}{T} + \left[\ln \frac{k_b}{h} + \frac{\Delta S_0^{\ddagger}}{R}\right].$$

The slope and intercept of $\ln k_m/T$ versus $1/T$ (Fig. 7) therefore provide $\Delta H_0^{\ddagger}$ and $\Delta S_0^{\ddagger}$, respectively (Table 1). $\Delta G_0^{\ddagger}$ could then be calculated at any particular temperature (Ta-

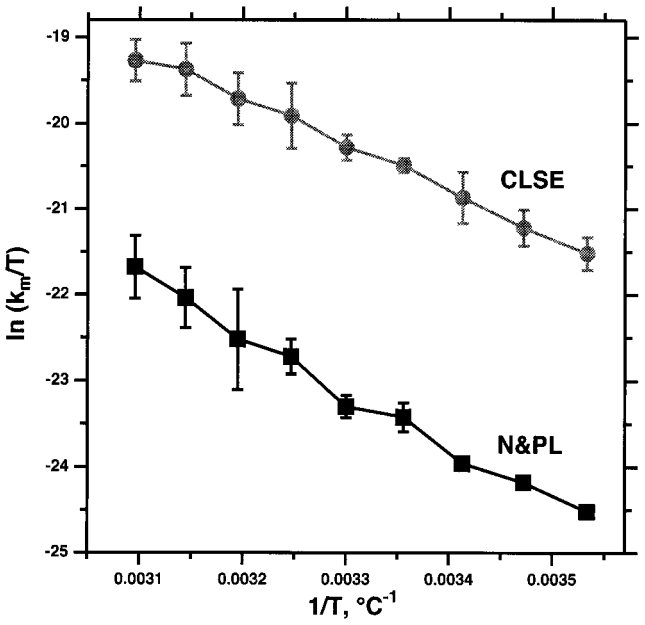

FIGURE 7 Determination of thermodynamic components of the activation barrier. The slope and intercept of linear regression equations to $\ln k_m/T$ versus $1/T$ for the measured rate constant k_m and the temperature T provide the basis for calculating $\Delta H_0^{\ddagger}$ and $\Delta S_0^{\ddagger}$, respectively. Mean ± SD averaged over measurements at six concentrations.

ble 1), although the variation over the range of temperatures considered was small. $-T \cdot \Delta S_0^{\ddagger}$ contributed the major component of $\Delta G_0^{\ddagger}$ for both preparations, constituting 55% for N&PL and 61% for CLSE at 37°C. The reduction in $\Delta G_0^{\ddagger}$ produced by the proteins, however, resulted from a change in $\Delta H_0^{\ddagger}$. The entropic contribution, $-T \cdot \Delta S_0^{\ddagger}$, increased minimally from 65 kJ/mole for the lipids alone to 68 kJ/mole in the presence of the proteins (Table 1). The proteins accelerated adsorption by lowering the enthalpy of transition with little change in entropy.

Our experiments also provided information concerning the later stages of adsorption. After the initial linear segment of the isotherm, the slope became steadily less negative until surface tension reached ~40–45 mN/m (Figs. 1 and 2). The curves at different concentrations became roughly parallel for N&PL, and, to a lesser extent, for CLSE. Below 40–45 mN/m, however, the kinetics of adsorption changed. In all experiments that reached 40 mN/m, the rate of fall in surface tension accelerated until reaching final constant surface tensions of ~25 mN/m. Only CLSE achieved surface tension below 40 mN/m appreciably before the end of the 35-min experiment, and, consequently, N&PL did not demonstrate this late acceleration.

TABLE 1 Thermodynamic Variables for Adsorption of N&PL and CLSE

	N&PL	CLSE
Reaction order	1.41 ± 0.18	1.73 ± 0.18
E_a (kJ/°K · mole)	56.6 ± 2.2	46.9 ± 1.1
$\Delta G_0^{\ddagger}$ (kJ/mole) at 37°C	119 ± 1	112 ± 2
$\Delta H_0^{\ddagger}$ (kJ/mole)	54.1 ± 2.2	44.4 ± 1.1
$\Delta S_0^{\ddagger}$ (J/°K · mole)	−211 ± 7	−220 ± 4
$-T \cdot \Delta S_0^{\ddagger}$ at 37°C (kJ/mole)	65.4 ± 2.2	68.2 ± 1.2

Data are mean ± SD.

DISCUSSION

Our experiments compare the adsorption of the complete set of lipids from calf surfactant with and without the native combination of SP-B and SP-C. Our analysis emphasizes the early stages of adsorption and, in particular, the initial fall in surface tension, but we also consider the unexpected acceleration late in this process.

Initial delay

Under conditions of low concentration and temperature that produce slow adsorption, surface tension falls only after an initial lag time. This interval has been observed previously (Clements, 1973; Morrow et al., 1993; Walters et al., 2000). The characteristics of the initial delay suggest that it represents merely the time required to reach the threshold surface concentration at which surface tension first begins to change. For the two preparations used in these studies, our calibration curves showed that the interfacial films affect surface tension only after surface concentration exceeds ~1.5 μmole/m^2. The alternative explanation, that some other process must occur before formation of the film can begin (Clements, 1973), would require that the delay exceed the interval expected for adsorption at the initial measurable rate to increase surface concentration from 0 to 1.5 μmole/m^2. Our data suggest just the opposite. Back extrapolation of the isotherm during the first fall in surface tension shows that adsorption at that rate would require more than the lag time to increase the surface concentration to the threshold of detection. These results suggest that the earliest rate of undetectable adsorption is faster than the first measurable rates, and that the progressive slowing of adsorption, which is evident from the isotherms (Fig. 1 and 2), extends to the region before the initial fall in surface tension. Adsorption is unmeasurable during this initial lag phase, but our data provide no imperative to invoke any process different from the mechanisms by which surfactant adsorbs when surface tension begins to drop.

Early stage

During the initial fall in surface tension, the temperature dependence of the rate constants shows that, for both preparations, the major component of the rate-limiting barrier is entropy (Table 1). This finding agrees with a priori expectation. The hydrophobic interactions that maintain bilayers

are based on entropy, resulting from the highly ordered clathrate cages formed by water around a nonpolar residue in an aqueous environment (Tanford, 1973). The transition of a bilayer to form an interfacial monolayer seems likely to require transient exposure of hydrophobic acyl groups to the aqueous solvent and consequently an unfavorable entropy of transition.

Prior measurements on complete canine surfactant agree with our results in some respects but differ in others (King and Clements, 1972). The magnitude of the rate-limiting barrier, 93 kJ/mole and 112 kJ/mole at 37°C for the complete dog and extracted calf samples, respectively, are similar. In both cases, $-T \cdot \Delta S_0^{\ddagger}$ is the major component of the barrier (King and Clements, 1972). The entropic barrier, however, is 60% larger for the native surfactant (108 kJ/mole) than for the extracts (68 kJ/mole). The enthalpy of transition for the two preparations actually diverge. For the extracted calf surfactant, the enthalpy of the rate-limiting structure is higher than for the dispersed vesicles ($\Delta H_0^{\ddagger} = 44$ kJ/mole), and enthalpy represents a major part of the barrier that slows adsorption. With the native canine surfactant, the rate-limiting complex actually has a lower enthalpy than the vesicles ($\Delta H_0^{\ddagger} < 0$). Extracted surfactant differs from the native material in that it lacks SP-A and that its structure is randomly assembled. The disparity in the thermodynamic results suggests that one or both of these differences between the native and extracted material causes adsorption to proceed by distinct mechanisms, although ultimately arriving at similar kinetics. The old observation that only native surfactant adsorbs via tubular myelin fits with different mechanisms. The similar biophysical function for surfactant with and without SP-A, whether in vitro (Hall et al., 1992) or in vivo (Korfhagen et al., 1996; Ikegami et al., 1998), fits with the ultimately similar kinetics.

The hydrophobic proteins accelerate adsorption not by reducing the major entropic barrier faced by the lipid vesicles but instead by reducing the enthalpy of activation (Table 1). $\Delta S_0^{\ddagger}$ is essentially unchanged. The lower $\Delta H_0^{\ddagger}$ could reflect an effect of the proteins on either the initial vesicles or the rate-limiting intermediate. $\Delta H_0^{\ddagger}$ gives only the difference in enthalpy between the two structures, and so the effect of the proteins could result from an alteration of either one. The proteins might destabilize the vesicles, or they could produce a catalytic reduction in the enthalpy of the intermediate. In either case, one likely source for a change in enthalpy would be an alteration of the Van der Waals interactions among the acyl chains.

The earliest models of how the proteins accelerate adsorption favored the possibility that the proteins destabilize the vesicles. Constituents other than dipalmitoylphosphatidylcholine (DPPC) were thought to disrupt interactions among lipids, resulting in more fluid structures that adsorbed and spread more rapidly. More recent evidence instead fits better with the stabilization of a crucial structure intermediate between vesicle and interface. Factors that accelerate adsorption when added to vesicles have the same effect when located exclusively at the interface. Both the surfactant proteins (Oosterlaken-Dijksterhuis et al., 1991a) and phospholipids other than DPPC (Walters et al., 2000) have this effect. For the phospholipids, the acceleration of adsorption is not just qualitatively in the same direction but quantitatively identical whether the material is added to vesicles or to a pre-existing interfacial film. These observations suggest that faster adsorption results from an effect on some structure equally accessible to vesicle and surface monolayer. For fusion of bilayer vesicles, mounting evidence supports the importance of a highly curved stalk intermediate between the two fusing vesicles (Chernomordik et al., 1987, 1999). The effect of phosphatidylethanolamines (PEs) suggests that a comparable structure may occur during fusion of a vesicle with an interfacial film. PEs, which favor the hexagonal H_{II} phase and lower the energy of lamellae concave toward the polar head group, accelerate both fusion and surfactant adsorption (Yu et al., 1984; Perkins et al., 1996), supporting the importance in both processes of a similarly bent structure. Separation of acyl groups required by tight curvature would disrupt van der Waals interactions and produce an unfavorable enthalpy (Fig. 8). In such a model, our results indicate that the essential effect of the proteins would be to minimize the unfavorable enthalpy.

The proteins accelerate adsorption almost to the maximum extent possible. At the higher temperatures, the proteins lower the activation barrier sufficiently that rates of adsorption approach diffusion-limitation. This limit in fact raises some caution in the interpretation of our results. Increased temperature also produces faster transport to the surface, and interpretation of a diffusion-limited process in terms of an activation barrier would lead to erroneous conclusions. The data for CLSE, however, argue against this possibility. The linear relationship of $\ln k_m/T$ to $1/T$ extends over the full range of temperatures with only minimal deviation at the highest temperatures at which k_d/k_m is lowest. Consequently, restricting the analysis to progressively lower temperatures, at which k_d/k_m is larger and measurements are less likely to reflect simple diffusion, had no effect on our qualitative results. The thermodynamic variables changed minimally, and in all cases, $\Delta H_0^{\ddagger}$ decreased relative to N&PL, with little change in $-T \cdot \Delta S_0^{\ddagger}$. Our conclusions therefore seem valid despite the progression with increasing temperature toward diffusion-limited adsorption.

Late stage

Our results also distinguish a late stage that is qualitatively distinct from the earlier process. At ~40–45 mN/m, the progressive slowing of the rate at which surface tension falls abruptly terminates, and adsorption accelerates until it reaches equilibrium values. This late acceleration is partic-

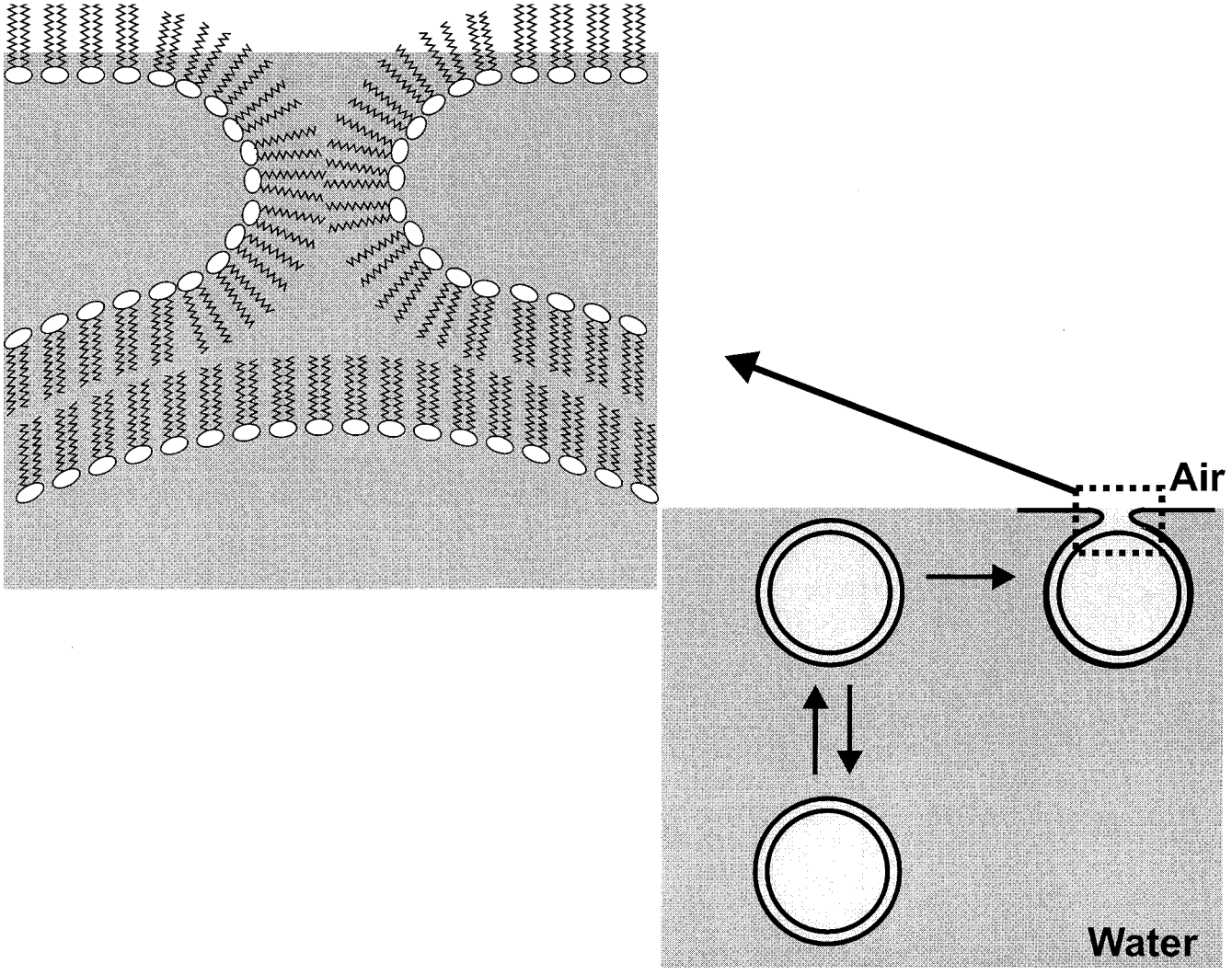

FIGURE 8 Model of the hypothetical rate-limiting structure intermediate between bilayer vesicles and interfacial monolayer. Enlarged view illustrates the separation of acyl chains required in such a structure that would produce an unfavorable $H_0^{\ddagger}$. The proteins would accelerate adsorption by reducing $H_0^{\ddagger}$ of this intermediate structure.

ularly interesting because of its physiological and pharmacological relevance. Following the creation of the air–liquid interface at birth, surfactant particles in most animals never again encounter an interface entirely devoid of material. Instead they insert into a surface expanded to the point that the density of the existing film drops below the equilibrium spreading value, allowing the addition of more material. The surface tensions at which this late acceleration occurs therefore represent values that surfactant, whether endogenous or exogenous, would encounter in the lung. All of our experiments that reached the threshold surface tension demonstrated the acceleration. This phenomenon is evident in some previously reported data (Notter et al., 1983; Oosterlaken-Dijksterhuis et al., 1991a) although not in others (Pérez-Gil et al., 1992; Walters et al., 2000). Because of its occurrence at a discrete surface tension, the late acceleration presumably reflects some interfacial change. Previous reports have shown that both the proteins (Oosterlaken-Dijksterhuis et al., 1991a) and the phospholipids (Walters et al., 2000) can produce faster adsorption when located either at the interface or in the vesicles, and the acceleration in our experiments could result from the accumulation of these factors in sufficient amounts to affect the rate from both locations. Several groups over the past decade have reported that more than a monolayer adsorbs to the interface (Hills, 1988; Oosterlaken-Dijksterhuis et al., 1991b; Schürch et al., 1995; Yu and Possmayer, 1996), and the late acceleration could reflect adsorption by this surface-associated material with behavior distinct from vesicles in the subphase. The inconsistency with which this late phase has been observed in previous studies (Notter et al., 1983; Oosterlaken-Dijksterhuis et al., 1991a; Pérez-Gil et al., 1992; Walters et al., 2000) suggests that it might reflect some unintended difference between experiments, such as different vesicles gen-

erated during resuspension. This possibility, however, in no way diminishes the importance of the phenomenon, particularly for the design of therapeutic surfactants.

CONCLUSIONS

In summary, our results show that, although the thermodynamic barrier to adsorption of the surfactant lipids is primarily the entropy of transition, the hydrophobic proteins accelerate adsorption by reducing the enthalpy of activation. Hypothetical mechanisms by which the proteins exert their effect must fit this constraint.

The authors thank Dr. Joseph McGuire for discussions of work in progress and the preliminary manuscript. The extracted calf surfactant (Infasurf) used in these studies was a gift from Dr. Edmund Egan of ONY, Inc.

This work was supported by HL 03502 and 54209, the Whitaker Foundation, and the American Lung Association of Oregon. Page charges were provided in part by the friends and family of Vern McKee.

REFERENCES

Ames, B. N. 1966. Assay of inorganic phosphate, total phosphate and phosphatases. *Methods Enzymol.* 8:115–118.

Arjomaa, P., and M. Hallman. 1988. Purification of a hydrophobic surfactant peptide using high-performance liquid chromatography. *Anal. Biochem.*171:207–212.

Borwankar, R. P., and D. T. Wasan. 1983. The kinetics of adsorption of surface active agents at gas–liquid surfaces. *Chem. Eng. Sci.* 38:1637–1649.

Chernomordik, L. V., G. B. Melikyan, and Y. A. Chizmadzhev. 1987. Biomembrane fusion: a new concept derived from model studies using two interacting planar lipid bilayers. *Biochim. Biophys. Acta.* 906: 309–352.

Chernomordik, L. V., E. Leikina, M. M. Kozlov, V. A. Frolov, and J. Zimmerberg. 1999. Structural intermediates in influenza haemagglutinin-mediated fusion. *Molec. Membr. Biol.* 16:33–42.

Clements, J. A. 1973. Composition and properties of pulmonary surfactant. *In* Respiratory Distress Syndrome, C.A. Villee, D. B. Villee, J. Zuckerman, editors. Academic Press, New York. 77–98.

Defay, R., and G. Pétré. 1971. Dynamic surface tension. *Surf. Colloid Sci.* 3:27–81.

Dukhin, S. S., G. Kretzschmar, and R. Miller. 1995. Dynamics of Adsorption at Liquid Interfaces: Theory, Experiment, Application. Elsevier, Amsterdam, New York.

Eyring, H. 1935. The activated complex and the absolute rate of chemical reactions. *Chem. Rev.* 17:65–77.

Galla, H.-J., N. Bourdos, A. von Nahmen, M. Amrein, and M. Sieber. 1998. The role of pulmonary surfactant protein C during the breathing cycle. *Thin Solid Films.* 329:632–635.

Hall, S. B., A. R. Venkitaraman, J. A. Whitsett, B. A. Holm, and R. H. Notter. 1992. Importance of hydrophobic apoproteins as constituents of clinical exogenous surfactants. *Am. Rev. Respir. Dis.* 145:24–30.

Hall, S. B., Z. Wang, and R. H. Notter. 1994. Separation of subfractions of the hydrophobic components of calf lung surfactant. *J. Lipid Res.* 35: 1386–1394.

Hawgood, S., B. J. Benson, J. Schilling, D. Damm, J. A. Clements, and R. T. White. 1987. Nucleotide and amino acid sequences of pulmonary surfactant protein SP 18 and evidence for cooperation between SP 18 and SP 28–36 in surfactant lipid adsorption. *Proc. Natl. Acad. Sci. U.S.A.* 84:66–70.

Hills, B. A. 1988. The Biology of Surfactant. Cambridge University Press, New York. 222–235.

Ikegami, M., T. R. Korfhagen, J. A. Whitsett, M. D. Bruno, S. E. Wert, K. Wada, and A. H. Jobe. 1998. Characteristics of surfactant from SP-A-deficient mice. *Am. J. Physiol. Lung Cell Mol Physiol.* 275:L247–L254.

Johannsen, E. C., J. B. Chung, C. H. Chang, and E. I. Franses. 1991. Lipid transport to air/water interfaces. *Colloids Surf.* 53:117–134.

Kaplan, R. S., and P. L. Pedersen. 1989. Sensitive protein assay in presence of high levels of lipid. *Methods Enzymol.* 172:393–399.

King, R. J., and J. A. Clements. 1972. Surface active materials from dog lung. III. Thermal analysis. *Am. J. Physiol.* 223:727–733.

Korfhagen, T. R., M. D. Bruno, G. F. Ross, K. M. Huelsman, M. Ikegami, A. H. Jobe, S. E. Wert, B. R. Stripp, R. E. Morris, S. W. Glasser, C. J. Bachurski, H. S. Iwamoto, and J. A. Whitsett. 1996. Altered surfactant function and structure in SP-A gene targeted mice. *Proc. Natl. Acad. Sci. U.S.A.* 93:9594–9599.

Kruger, P., M. Schalke, Z. Wang, R. H. Notter, R. A. Dluhy, and M. Lösche. 1999. Effect of hydrophobic surfactant peptides SP-B and SP-C on binary phospholipid monolayers. *Biophys. J.* 77:903–914.

Liggieri, L., F. Ravera, and A. Passerone. 1996. A diffusion-based approach to mixed adsorption kinetics. *Colloids Surf. A.* 114:351–359.

Lipp, M. M., K. Y. C. Lee, J. A. Zasadzinski, and A. J. Waring. 1996. Phase and morphology changes in lipid monolayers induced by SP-B protein and its amino-terminal peptide. *Science.* 273:1196–1199.

Longo, M. L., A. M. Bisagno, J. A. Zasadzinski, R. Bruni, and A. J. Waring. 1993. A function of lung surfactant protein SP-B. *Science.* 261:453–456.

Morrow, M. R., J. Perez-Gil, G. Simatos, C. Boland, J. Stewart, D. Absolom, V. Sarin, and K. M. Keough. 1993. Pulmonary surfactant-associated protein SP-B has little effect on acyl chains in dipalmitoylphosphatidylcholine dispersions. *Biochemistry.* 32:4397–4402.

Nogee, L. M. 1998. Genetics of the hydrophobic surfactant proteins. *Biochim. Biophys. Acta.* 1408:323–333.

Notter, R. H., J. N. Finkelstein, and R. D. Taubold. 1983. Comparative adsorption of natural lung surfactant, extracted phospholipids, and artificial phospholipid mixtures to the air–water interface. *Chem. Phys. Lipids.* 33:67–80.

Oosterlaken-Dijksterhuis, M. A., H. P. Haagsman, L. M. G. van Golde, and R. A. Demel. 1991a. Interaction of lipid vesicles with monomolecular layers containing lung surfactant proteins SP-B or SP-C. *Biochemistry.* 30:8276–8281.

Oosterlaken-Dijksterhuis, M. A., H. P. Haagsman, L. M. G. van Golde, and R. A. Demel. 1991b. Characterization of lipid insertion into monomolecular layers mediated by lung surfactant proteins SP-B and SP-C. *Biochemistry.* 30:10965–10971.

Pérez-Gil, J., J. Tucker, G. Simatos, and K. M. Keough. 1992. Interfacial adsorption of simple lipid mixtures combined with hydrophobic surfactant protein from pig lung. *Biochem. Cell Biol.* 70:332–338.

Perkins, W. R., R. B. Dause, R. A. Parente, S. R. Minchey, K. C. Neuman, S. M. Gruner, T. F. Taraschi, and A. S. Janoff. 1996. Role of lipid polymorphism in pulmonary surfactant. *Science.* 273:330–332.

Schürch, S., R. Qanbar, H. Bachofen, and F. Possmayer. 1995. The surface-associated surfactant reservoir in the alveolar lining. *Biol. Neonate.* 67(suppl):61–76.

Searcy, R. L., and L. M. Bergquist. 1960. A new color reaction for the quantitation of serum cholesterol. *Clin. Chim. Acta.* 5:192–199.

Taneva, S., and K. M. W. Keough. 1994a. Pulmonary surfactant proteins SP-B and SP-C in spread monolayers at the air-water interface: I. Monolayers of pulmonary surfactant protein SP-B and phospholipids. *Biophys. J.* 66:1137–1148.

Taneva, S., and K. M. W. Keough. 1994b. Pulmonary surfactant proteins SP-B and SP-C in spread monolayers at the air-water interface: II. Monolayers of pulmonary surfactant protein SP-C and phospholipids. *Biophys. J.* 66:1149–1157.

Taneva, S., and K. M. W. Keough. 1994c. Pulmonary surfactant proteins SP-B and SP-C in spread monolayers at the air–water interface: III. Proteins SP-B plus SP-C with phospholipids in spread monolayers. *Biophys. J.* 66:1158–1166.

Tanford, C. 1973. The Hydrophobic Effect: Formation of Micelles and Biological Membranes. Wiley, New York.

Tokieda, K., J. A. Whitsett, J. C. Clark, T. E. Weaver, K. Ikeda, K. B. McConnell, A. H. Jobe, M. Ikegami, and H. S. Iwamoto. 1997. Pulmonary dysfunction in neonatal SP-B-deficient mice. *Am. J. Physiol. Lung Cell Mol Physiol.* 273:L875–L882.

Veldhuizen, E. J., and H. P. Haagsman. 2000. Role of pulmonary surfactant components in surface film formation and dynamics. *Biochim. Biophys. Acta.* 1467:255–270.

Walters, R. W., R. R. Jenq, and S. B. Hall. 2000. Distinct steps in the adsorption of pulmonary surfactant to an air–liquid interface. *Biophys. J.* 78:257–266.

Wang, Z., S. B. Hall, and R. H. Notter. 1995. Dynamic surface activity of films of lung surfactant phospholipids, hydrophobic proteins, and neutral lipids. *J. Lipid Res.* 36:1283–1293.

Wang, Z., S. B. Hall, and R. H. Notter. 1996. Roles of different hydrophobic constituents in the adsorption of pulmonary surfactant. *J. Lipid Res.* 37:790–798.

Ward, A. F. H., and L. Tordai. 1946. Time-dependence of boundary tensions of solutions. I. The role of diffusion in time-effects. *J. Chem. Phys.* 14:453–461.

Warr, R. G., S. Hawgood, D. I. Buckley, T. M. Crisp, J. Schilling, B. J. Benson, P. L. Ballard, J. A. Clements, and R. T. White. 1987. Low molecular weight human pulmonary surfactant protein (SP5): isolation, characterization, and cDNA and amino acid sequences. *Proc. Natl. Acad. Sci. U.S.A.* 84:7915–7919.

Whitsett, J. A., B. L. Ohning, G. Ross, J. Meuth, T. Weaver, B. A. Holm, D. L. Shapiro, and R. H. Notter. 1986. Hydrophobic surfactant-associated protein in whole lung surfactant and its importance for biophysical activity in lung surfactant extracts used for replacement therapy. *Ped. Res.* 20:460–467.

Yu, S.-H., P. G. R. Harding, and F. Possmayer. 1984. Artificial pulmonary surfactant. Potential role for hexagonal H(II) phase in the formation of a surface-active monolayer. *Biochim. Biophys. Acta.* 776:37–47.

Yu, S. H., and F. Possmayer. 1990. Role of bovine pulmonary surfactant-associated proteins in the surface-active property of phospholipid mixtures. *Biochim. Biophys. Acta.* 1046:233–241.

Yu, S. H., and F. Possmayer. 1996. Effect of pulmonary surfactant protein A and neutral lipid on accretion and organization of dipalmitoylphosphatidylcholine in surface films. *J. Lipid Res.* 37:1278–1288.